Epithelial Cell Transforming Protein 2 (ECT2) Depletion Blocks Polar Body Extrusion and Generates Mouse Oocytes Containing Two Metaphase II Spindles

Judith Elbaz, Yitzhak Reizel, Nava Nevo, Dalia Galiani, and Nava Dekel

Department of Biological Regulation, The Weizmann Institute of Science, Rehovot 76100, Israel

Completion of the first meiosis in oocytes is achieved by the extrusion of the first polar body (PBI), a particular example of cell division. In mitosis, the small GTPase RhoA, which is activated by epithelial cell transforming protein 2 (ECT2), orchestrates contractile ring constriction, thus enabling cytokinesis. However, the involvement of this pathway in mammalian oocytes has not been established. To characterize the role of ECT2 in PBI emission in mouse oocytes, the small interfering RNA approach was employed. We found that ECT2 depletion significantly reduces PBI emission, induces first metaphase arrest, and generates oocytes containing two properly formed spindles of the second metaphase. Moreover, we describe, for the first time, that before PBI emission, RhoA forms a ring that is preceded by a dome-like accumulation at the oocyte cortex, next to the spindle. This unique mode of RhoA translocation failed to occur in the absence of ECT2. We further found that the Rho-dependent kinase, a main RhoA effector, is essential for PBI emission. In addition, we demonstrate herein that ECT2 is subjected to phosphorylation/dephosphorylation throughout meiosis in oocytes and further reveal that PBI emission is temporally associated with ECT2 dephosphorylation. Our data provide the first demonstration that an active cyclin-dependent kinase 1, the catalytic subunit of the maturation-promoting factor, phosphorylates ECT2 during the first meiotic metaphase and that cyclin-dependent kinase 1 inactivation at anaphase allows ECT2 dephosphorylation. In conclusion, our study demonstrates the indispensable role of the maturation-promoting factor/ECT2/RhoA pathway in PBI extrusion in mouse oocytes. (***Endocrinology*** **151: 755–765, 2010)**

Sexual reproduction involves the fusion of two haploid gametes, the oocyte and the spermatozoon, both products of meiotic divisions. In mammalian oocytes, meiosis is initiated during embryonic life, proceeds up to the diplotene stage of the first prophase, and arrests around birth. Throughout meiotic arrest, the chromosomes are diffused and surrounded by a nuclear membrane, known as the germinal vesicle (GV). Meiosis, which is reinitiated at the onset of puberty in a selected number of oocytes at each reproductive cycle, consists of GV breakdown (GVB), chromosome condensation, and formation of the first meiotic metaphase (MI) spindle. The first meiosis is completed by an asymmetric division producing the oocyte and the first polar body (PBI).

The master regulator of meiosis is the maturation-promoting factor (MPF), the components of which are the catalytic cyclin-dependent kinase 1 (CDK1) and the regulatory cyclin B1 (1–3). The inactive CDK1 in meiotically arrested oocytes is gradually activated upon reinitiation of meiosis, followed by a sharp transient inactivation and a further reactivation (4–6). CDK1 inactivation takes place at the onset of anaphase I and is subsequent to degradation of cyclin B1 (7), which is brought about by the ubiquitin-dependent proteasomal proteolysis (8). We previously showed that the artificial maintenance of CDK1 activity at the onset of anaphase totally blocks PBI emission (9). However, the molecular events downstream to CDK1 inactivation that allow the formation of PBI emission are yet unknown.

ISSN Print 0013-7227 ISSN Online 1945-7170
Printed in U.S.A.

doi: 10.1210/en.2009-0830 Received July 27, 2009. Accepted October 30, 2009.
First Published Online December 8, 2009

Abbreviations: CDK1, Cyclin-dependent kinase 1; DAPI, 4′,6-diamidino-2-phenylindole; ECT2, epithelial cell transforming protein 2; FBS, fetal bovine serum; GV, germinal vesicle; GVB, GV breakdown; MI, first meiotic metaphase I; MII, second meiotic metaphase II; MPF, maturation-promoting factor; PBI, first polar body; PDE, phosphodiesterase; PMSG, pregnant mare serum gonadotropin; ROCK, Rho-dependent kinase; siRNA, small interfering RNA.

PBI emission is a particular case of cytokinesis, a process executed by the constriction of the actomyosin-based contractile ring (10–12). This ring enables furrow ingression, and subsequent abscission, leading to complete separation of daughter cells (reviewed in Ref. 13). RhoA small GTPase induces constriction of the contractile ring via three main effectors as follows: it promotes the polymerization of actin necessary for contractile ring formation through the formin family (14); it phosphorylates myosin II light chain, which generates the force required for the contractile ring ingression through the Rho-dependent kinase (ROCK) (15, 16); and it regulates late steps of abscission through citron kinase (12) (reviewed in Ref. 17). In somatic cells, the presence of RhoA during mitosis is absolutely essential for both furrow formation and ingression (10, 18, 19). Furthermore, induction of actomyosin constriction requires local accumulation and activation of RhoA at the equatorial cortex (20–23).

Like most small G proteins, RhoA is a molecular switch that cycles between resting GDP-bound and active GTP-bound states. The epithelial cell transforming protein 2 (ECT2) is the guanine nucleotide exchange factor that activates RhoA in dividing epithelial cells. Specifically, ECT2 directs the precise localization of RhoA at the equatorial cortex by its accumulation at the midzone, a structure formed between segregated chromatids at the onset of anaphase. Upon ECT2 inhibition in somatic cells, RhoA fails to accumulate at the cell cortex, cytokinesis does not occur, and multinucleated cells are formed (21, 22, 24–28). ECT2, which is known to be regulated by phosphorylation, was reported to be phosphorylated during G2 and M phases in HeLa cells (28). Later studies showed that ECT2 is dephosphorylated during cytokinesis (23, 29).

It was recently shown in *Xenopus* oocytes that ECT2 controls RhoA localization and PBI emission (30). However, the signaling cascade of ECT2, as well as the phenotype of ECT2-depleted oocytes, was not examined. In the present study, we report that ECT2 is essential for the ring-shaped accumulation of RhoA, without which PBI does not form. Some oocytes that failed to extrude PBI contained two distinct spindles of the second meiotic metaphase (MII), a phenomenon that is actually analogous to binucleation reported in somatic cells. Finally, we show for the first time that MPF inactivation at the metaphase-to-anaphase transition brings about ECT2 dephosphorylation.

Materials and Methods

Reagents

Leibovitz's L-15 tissue culture medium and fetal bovine serum (FBS) were purchased from Biological Industries (Kibbutz Beit Hemeek, Israel). Antibiotics were purchased from Bio-Lab Ltd. (Jerusalem, Israel), pregnant mare's serum gonadotropin (PMSG) from Chronogest Intervet (Boxmeer, The Netherlands) and ovine LH (o-LH-26) from National Hormone and Pituitary Program (Harbor-UCLA Medical Center, Torrance, CA). The ROCK inhibitor Y27632 was purchased from Calbiochem (San Diego, CA), MG132, and cilostamide from Alexis Biochemicals (San Diego, CA) and roscovitine from LC Laboratories (Woburn, MA). Protease inhibitor cocktail, phenylmethylsulfonyl fluoride, leupeptin, and pepstatin as well as anti-β-tubulin and fluorescein isothiocyanate-conjugated anti-α-tubulin monoclonal antibodies were from Sigma-Aldrich Corp. (St Louis, MO). Anti-RhoA, anti-ECT2 and anti-general ERK1/2 antibodies were purchased from Santa Cruz Biotechnology Inc. (Santa Cruz, CA; sc-418, sc-1005, and sc-135900, respectively) and Cy3-conjugated goat antimouse $F(ab)'_2$ IgG antibodies from Jackson ImmunoResearch Laboratories (West Grove, PA). 4′,6-Diamidino-2-phenylindole (DAPI) stain was purchased from Molecular Probes (Eugene, OR).

Animals

Sexually immature C57BL/6 female mice (25 d old) were purchased from Harlan Laboratories (Rehovot, Israel) and handled according to the guidelines of the National Institutes of Health and of the Weizmann Institute for management of laboratory animals. This study was approved by the institutional animal care and use committee. The mice were housed in a light- and temperature-controlled room, with food and water provided *ad libitum*.

Oocytes collection and culture

The aforementioned mice, sc injected with 5 IU PMSG for induction of follicular development and sacrificed 48 h later, were used. The ovaries were removed and placed in L-15 medium, supplemented with 5% FBS, penicillin (100 IU/ml), and streptomycin (100 mg/ml). To maintain the oocytes in meiotic arrest, the phosphodiesterase 3A (PDE3A)-specific inhibitor cilostamide (7.5 mM) was included in the medium of incubation (31). The large antral follicles were punctured under a stereoscopic microscope to release the cumulus-oocyte complexes. Cumulus cells were removed by repetitive pipetting, and the denuded fully grown oocytes were incubated in a 37 C humidified incubator. Oocytes were examined for maturation and PBI emission using a stereoscopic microscope (SMZ 1500; Nikon, Tokyo, Japan).

Small interfering RNA (siRNA) microinjection

Oocytes collected as mentioned above were denuded and incubated in a cilostamide-containing medium. They were transferred to 10-μl drops, under 3.5 ml of paraffin oil in a 35-mm Falcon petri dish. Dishes were placed on a heated stage (28 C) of an inverted microscope equipped with differential interference contrast optics (Axiovert 35; Zeiss, Oberkochen, Germany). Oocytes were microinjected with ECT2 siRNA as well as nontargeting scrambled siRNA (approximately 10 pl) using a three-dimensional motor coarse control micromanipulator (Eppendorf, Hamburg, Germany). The siRNA pools were purchased from Dharmacon (Lafayette, CO): ECT2 siGENOME SMARTpool, catalog no. M-045026-00 NM_007900) and nontargeting siGENOME (pool number 2). Noninjected oocytes served as a control for the effect of the microinjection.

RNA extraction and cDNA preparation

Liquid nitrogen-frozen oocytes were homogenized in 500 μl Tri-Reagent (Sigma-Aldrich) through a 21-gauge syringe. Glycogen (10 μl) (Roche Applied Science, Mannheim, Germany) was added to allow better precipitation of RNA. After adding 100 μl chloroform to allow phase separation by centrifugation (at 4 C), 250 μl ispropanol was added to the aqueous phase. After several hours in −20 C, the RNA was precipitated by centrifugation. The pellet was washed in cold 70% ethanol and then dried. The RNA pellet was resuspended, and deoxyribonuclease treatment was performed according to the manufacturer's instructions (Ambion, Austin, TX). Quality and quantity of total RNA extracted were assessed using a Nanodrop spectrophotometer. RNA samples (200 ng) were reverse transcribed using recombinant reverse transcriptase (Moloney murine leukemia virus; Promega, Madison, WI) and oligo-deoxythymidine primer, as indicated in the manufacturer's protocol. The cDNA was then diluted two times.

Semiquantitative PCR

The reverse-transcribed diluted cDNA was amplified by PCR. The nucleotide sequences are as follows: RhoA (NM_016802), CCAGAAAGGCCCAAGTCCA and TGAGAAAGGCTATGCCACCT; RhoB (NM_007483), CGAACTTTGTGCCTGTCCTAC and CCTGTTGCCTTCCTTTACCA; RhoC (NM_007484), TCCTCAACCCTCCCACCTT and GCTACTACCCAAAGCAGAAACC; PDE3A (NM_018779), ATGGGTAGAGCGAGCTGTGT and ACCTTGTGGAGTCAGGCATC; PDE4D (NM_011056), CATGTCGAAGCACATGAACC and ACTCACGATTGTCCTCCAA. The primers were designed using the Primer3 program and validated for their specificity by the NCBI-BLAST program. PCR was performed in 25-μl reaction volumes containing 2 μl cDNA, 5 pmol each primer, and 5 μl ReddyMix PCR Master Mix (ABgenehouse, Epsom, Surrey, UK).

Protein extraction and Western blot analysis

Oocytes were lysed in RIPA buffer supplemented with 1 mM phenylmethylsulfonyl fluoride, 10 μg/ml leupeptin, 2 μg/ml pepstatin, protease inhibitor (according to manufacturer's instructions), and 400 μM $NaVO_3$. After pipetting, the lysates were kept on ice for 30 min and then centrifuged for 20 min, after which the supernatants were collected. The samples were dissolved in protein sample buffer [2% β-mercaptoethanol, 2% sodium dodecyl sulfate, 50 mm Tris, HCl (pH 6.8), 10% glycerol, and 0.01% bromophenol blue), boiled, and loaded onto 10% SDS-PAGE. For better resolution of the ECT2 phosphorylation shift, 8% SDS-PAGE was used, and the bisacrylamide in the monomer mixture was reduced from 8 to 0.12%. After electrophoretic separation, the proteins were transferred to polyvinylidene fluoride membranes (Millipore, Billerica, MA), which were washed for 1 h with a blocking solution (5% milk, 0.05% Tween in PBS) and then incubated with primary antibodies (over night, 4 C) and antirabbit horseradish peroxidase-conjugated antibodies (1:4000 for 1 h at room temperature). Chemiluminescent signals were generated by incubation with the enhanced chemiluminescence reagent (Amersham, Buckinghamshire, UK). For quantification, intensity values of bands were measured from three different repeats using image J (National Institutes of Health, Bethesda, MD).

Immunofluorescence

The oocytes were fixed in ice-cold 10% trichloroacetic acid in distilled water for 15 min (32) followed by extensive washing with GB-PBS (PBS containing 10 mg/ml BSA and 10 mM glycine, pH 7.4), permeabilization in Triton X-100 (1% in PBS) for 4 min, and transfer to blocking solution (GB-PBS containing 10% FBS) for 1 h. The oocytes were then incubated overnight with RhoA primary antibodies, extensively washed, and further incubated with the secondary antibodies, cy3 goat antimouse F(ab)′ (1:200) for 2 h. They were then incubated in fluorescein isothiocyanate-conjugated tubulin antibodies (1:100) and DAPI for 2 h, washed, and mounted in elvanol on silicone-coated glass slides and covered by coverslips resting on a silicone ring containing 100-mm glass beads that served as spacers. The oocytes were visualized using an LSM710 confocal microscope (Zeiss). In some oocytes, serial images were acquired at different planes along the z-axis (Z-stack acquisition). From these serial images, a three-dimensional picture was generated using Zeiss's ZEN 2008 software.

Results

ECT2 depletion blocks PBI extrusion

To examine the necessity of ECT2 for PBI extrusion, denuded oocytes, which were incubated with cilostamide to keep them meiotically arrested, were microinjected with either ECT2 or nontargeting scrambled siRNA. Noninjected oocytes served as a control for the effect of this manipulation. Meiotic arrest was maintained for 24 h, after which cilostamide was washed, and the oocytes were allowed to undergo spontaneous maturation. The oocytes were monitored for the presence of PBI after an additional 24 h. Semiquantitative RT-PCR and Western blot analysis revealed that ECT2 levels were substantially downregulated, demonstrating high efficiency of the siRNA treatment (Fig. 1, A and B). Microscopic examination revealed that the fraction of oocytes extruding PBI after ECT2 depletion was reduced by 57% compared with scrambled siRNA-injected oocytes (24.1%, n = 421; 55.7%, n = 373, respectively; two way ANOVA P = 0.0032) (Fig. 1C). Interestingly, some of the ECT2 siRNA-injected oocytes that failed to extrude PBI exhibited a cytoplasmic elongated protrusion (18.9 *vs.* 4.5% in scrambled siRNA-injected oocytes, Fig. 1, D and Ec). The formation of these protrusions suggests that these oocytes may have initiated, but failed to complete, the process of cytokinesis. The microinjection itself did not affect the experimental outcome (Fisher's least significant difference).

ECT2 depletion induces MI arrest and generates oocytes containing two MII spindles

To examine their chromosomal configuration, ECT2 siRNA-injected oocytes were fixed 24 h after the initiation of spontaneous maturation and stained with antitubulin antibodies as well as with the DAPI fluorescent DNA

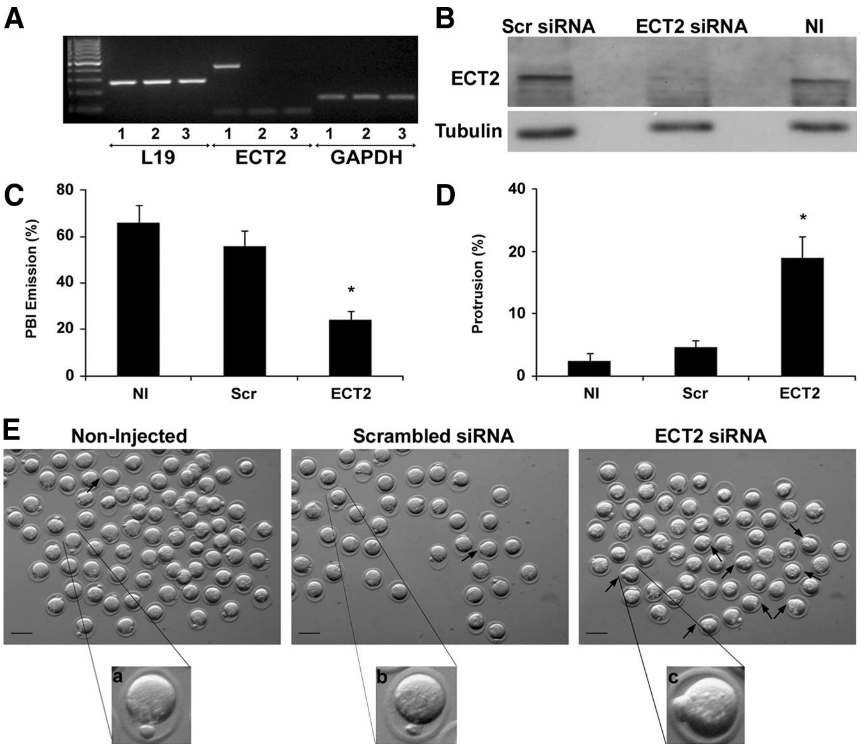

FIG. 1. Inhibition of PBI extrusion and formation of an elongated protrusion after ECT2 siRNA intraoocyte microinjection. Denuded mouse oocytes maintained meiotically arrested in a cilostamide-containing L-15 tissue culture medium were microinjected with scrambled or ECT2 siRNA. Cilostamide was washed after 24 h, and the oocytes were allowed to undergo spontaneous maturation. A, Total RNA was extracted from oocytes 24 and 48 h after ECT2 siRNA microinjection (lanes 2 and 3, respectively) as well as from scrambled siRNA-injected oocytes (lanes 1). Semiquantitative RT-PCRs were performed to generate ECT2 cDNAs from these oocytes. Both L19 and glyceraldehyde-3-phosphate dehydrogenase (GAPDH) housekeeping genes were used for normalization. The presented results represent one of three similar independent experiments. B, The proteins from oocytes injected with scrambled siRNA (scr) and ECT2 siRNA as well as noninjected (NI) oocytes were extracted after 48 h incubation and subjected to Western blot analysis. To obtain a sufficient amount of protein, the oocytes from three independent experiments were pooled. Each lane contains proteins extracted from 200 oocytes. C, The microinjected oocytes were monitored for PBI extrusion. *, $P = 0.0032$ [two-way ANOVA $F_{(2,8)} = 33.14$]. D, The same oocytes were scored for the presence of elongated protrusions. *, $P = 0.01$ [two-way ANOVA $F_{(2,8)} = 17.9$]. C and D show the means ± SE of four independent experiments with approximately 100 oocytes per group. E, A representative photograph of each group of oocytes 48 h after injection. The *black arrows* indicate the oocytes that failed to extrude PBI and exhibited an elongated protrusion. *Bars*, 100 μm.

probe. In some oocytes, serial images were acquired at different planes along the z-axis, and a three-dimensional picture was generated. As expected, most of the control oocytes were arrested at the second metaphase and contained a typical MII spindle (Fig. 2A, f1 and f2). However, in the ECT2-depleted oocytes, several abnormal phenotypes were detected. The most remarkable phenotype was that of oocytes containing two properly formed MII spindles, described here for the first time (Fig. 2A, a1–a3, and supplemental Fig. 1, published as supplemental data on The Endocrine Society's Journals Online web site at http://endo.endojournals.org). In these oocytes, the homologous chromosomes successfully segregated; nevertheless, because PBI emission failed, the set of chromosomes that should have been expelled was trapped within the oocyte. Interestingly, the progression to MII still occurred and each set of chromosomes arranged at the equator of the newly formed MII spindle. Each of the two spindles was aligned in parallel to the cortex, resembling the orientation of a single MII spindle during normal second metaphase arrest. Other oocytes seem to be arrested at MI (Fig. 2A, b1–b3), some of which contained partially or totally segregated chromosomes attached to the spindle poles (Fig. 2A, c1–c3 and d1–d3). Quantification of these configurations revealed that 23.5% of the ECT2-depleted oocytes contained two well-formed MII spindles, whereas this phenotype was not observed in control oocytes (n = 210 and n = 192, respectively; $P = 0.02$) (Fig. 2B). About half (48.2%) of the ECT2-depleted oocytes failed to complete homologous chromosome segregation, a phenotype observed in only 18.6% of the scrambled siRNA-injected oocytes ($P = 0.02$). Some of the ECT2-depleted oocytes that contained a metaphase-like spindle displayed partially segregated chromosomes (37.8%); no partial DNA segregation was observed in control oocytes ($P = 0.01$) (Fig. 2A, c1–c3). About 25% of the ECT2-depleted oocytes contained a single typical MII spindle, which is consistent with the fraction of these oocytes that extruded PBI (24.1%, Fig. 1C).

RhoA expression and localization in mouse oocytes

Mammalian cells express three main isoforms of Rho proteins: RhoA, RhoB, and RhoC. To characterize their expression, RNA was extracted from mouse oocytes and cDNA was synthesized and subjected to PCR. For comparison, PCRs were also performed on cDNA from whole ovaries. A possible cross-contamination was ruled out by the use of two control genes: PDE3A, an oocyte-specific gene, and PDE4D, a granulosa-specific PDE isoform. We found that RhoA and RhoB are expressed in mouse oocytes, whereas RhoC mRNA is absent (Fig. 3A). Intact ovaries, however, expressed all three isoforms. Because RhoA is the isoform that plays a major role in cytokinesis in somatic cells, its localization during PBI emission was next determined. Mouse oocytes were continuously monitored between 10 and 14 h of their spon-

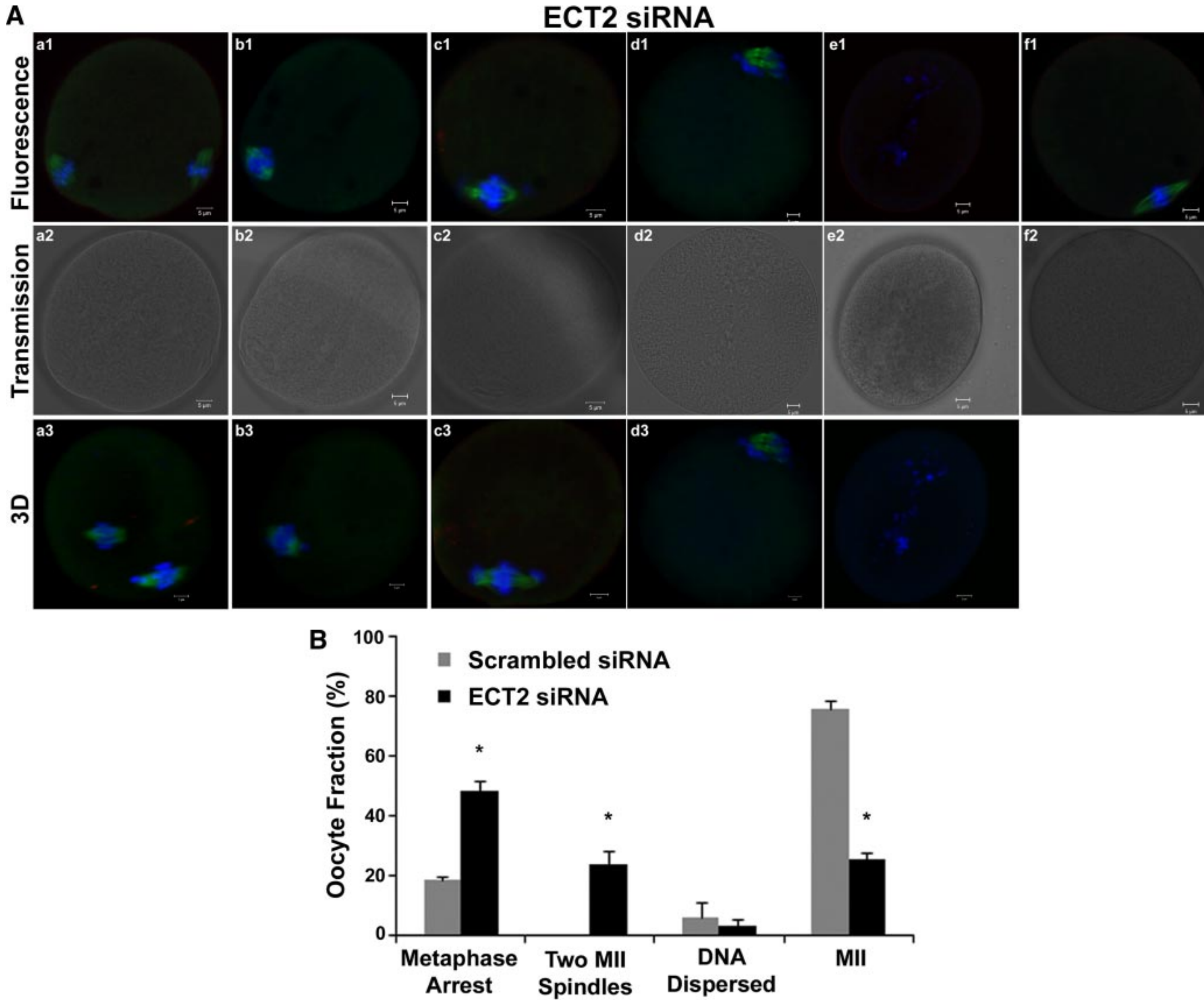

FIG. 2. Spindle/chromosome configuration in the ECT2-depleted oocytes. A, ECT2 siRNA-microinjected oocytes were fixed 24 h after their release from meiotic arrest. They were stained using tubulin (*green*) antibodies as well as DAPI (*blue*) fluorescent DNA probe and monitored by an LSM710 Zeiss confocal microscope. a, An oocyte containing two MII spindles; b, meiotic arrest at MI stage; c and d, the homologous chromosomes have partially/totally segregated but they are still attached to the spindle; e, DNA dispersed all over the oocyte; f, an oocyte that had extruded PBI and contains a regular MII spindle, similar to control. B, Quantification of the different chromosomal configurations in the ECT2-depleted oocytes. *, $P < 0.05$. 3D, Three-dimensional.

taneous maturation and fixed at PBI emission. They were subsequently stained using anti-RhoA and antitubulin antibodies as well as DAPI. We show herein, for the first time in mammalian oocytes, a distinct pattern of RhoA accumulation at the cortical region, adjacent to the spindle (Fig. 3B). Specifically, during meiotic arrest, RhoA is distributed uniformly on the cortex of the oocyte (Fig. 3B, a1–a3). After the organization of the spindle, RhoA translocates to a relatively large area of the membrane surface, forming a dome-like structure in the vicinity of the spindle (Fig. 3B, b1–b3, and supplemental Fig. 2). This structure is later remodeled into a ring at the shoulders of the protrusion, marking the cortical region for subsequent meiotic furrow formation (Fig. 3B, c–e, and supplemental Fig. 3). The RhoA ring then shrinks around the spindle center, enabling separation of the homologous chromosomes and PBI emission (Fig. 3B, f1–f3, and supplemental Fig. 4). It finally appears as a dot at the region of the polar body and the oocyte membrane apposition. Unexpectedly, most oocytes exhibited a spindle oriented parallel, and not perpendicular, to the cortex. At initial stages of outpocketing, the entire spindle was localized within the protrusion, between the forming contractile ring and the oocyte cortex (Fig. 3B, e1–e3; supplemental Fig. 5 and Fig. 3). It is only after membrane constriction that the spindle becomes perpendicular to the cortex (Fig. 3B, f1–f3).

ECT2 is essential for RhoA translocation

The requirement of ECT2 for RhoA translocation was next assessed. For this purpose, the previously described

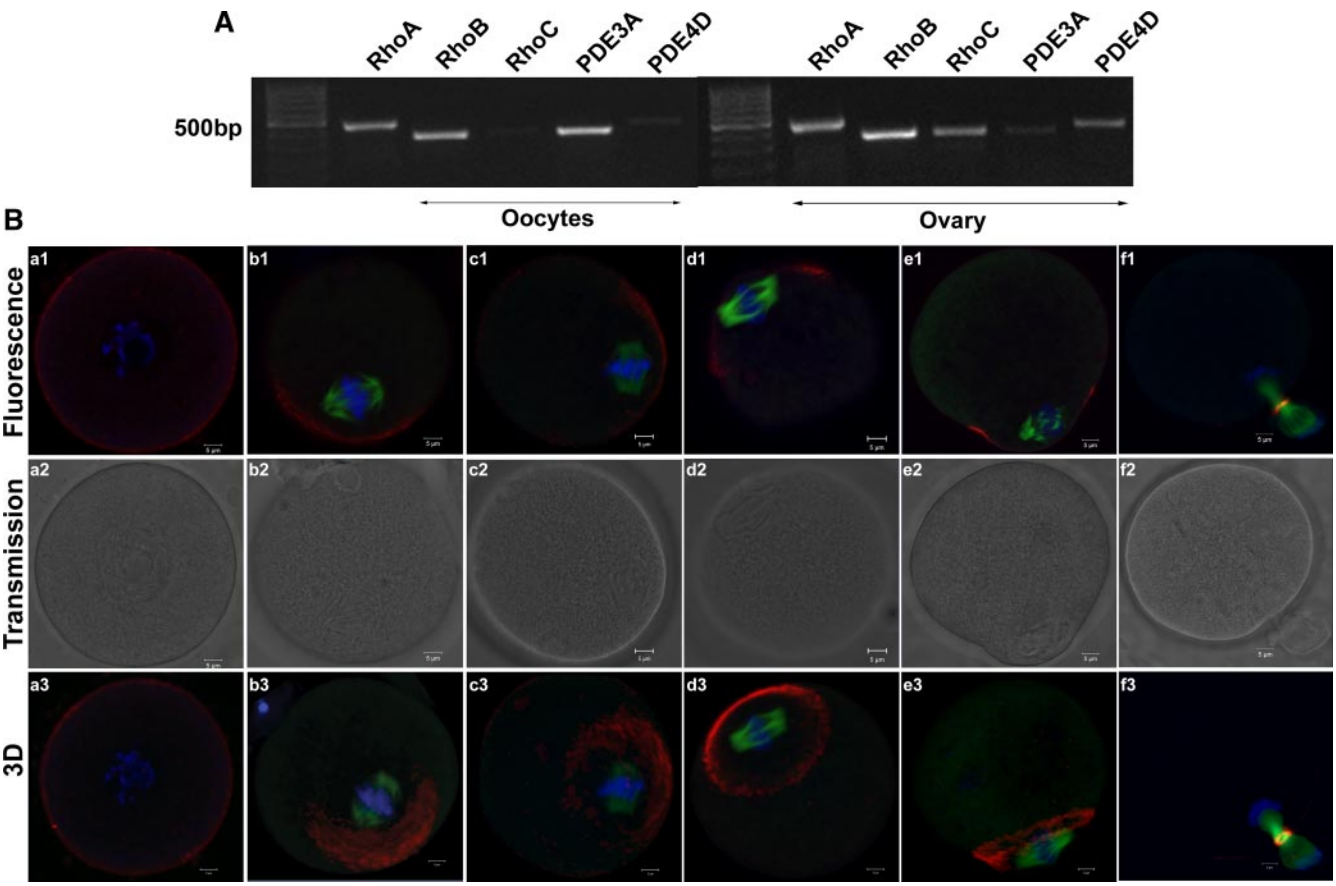

FIG. 3. Expression of the Rho isoforms in mouse oocytes and ovaries and RhoA localization in oocyte during PBI emission. A, RT-PCR for RhoA, RhoB, RhoC, PDE3A, and PDE4D mRNAs was performed in oocytes and whole ovaries of PMSG-primed 25-d-old female mice. In the oocyte sample, PDE3A serves as a positive control and PDE4D as a negative control, whereas both genes should be expressed in the ovary sample. PCR was performed as described in *Materials and Methods*, and reactions were subjected to 39 cycles for RhoA, -B, and -C and 33 cycles for PDE3A and -4D. The results of one of three similar experiments are presented. B, Oocytes were fixed during PBI emission, 12 h after initiation of spontaneous maturation. They were stained using RhoA (*red*) and tubulin (*green*) antibodies as well as by DAPI (*blue*) and monitored by an LSM710 Zeiss confocal microscope. a, A meiotically arrested GV oocyte displaying a membrane distribution of RhoA; b, at MI, RhoA accumulates in a dome-shaped manner at the cortical region that is adjacent to the spindle; c, a space begins to form in the dome-shaped RhoA accumulation; d, the RhoA accumulation is remodeled into a ring even before the cortex starts to constrict; e, the entire spindle is located in the upcoming PBI and is positioned parallel to the cortex, and RhoA is restricted to the shoulders of the protrusion; f, during late cytokinesis, the RhoA ring narrows and finally constricts to form a dot.

ECT2 siRNA-microinjected oocytes, which were allowed to undergo spontaneous maturation, were fixed during PBI emission and stained with anti-RhoA and antitubulin antibodies as well as DAPI. A considerable difference in RhoA localization was observed between the control and the ECT2 siRNA-treated groups. In scrambled siRNA-injected oocytes, RhoA localization was similar to that observed in nontreated oocytes (n = 75, Fig. 4, e–f). However, in the ECT2 siRNA-injected oocytes, RhoA was not detected (n = 64, Fig. 4, a and b). Interestingly, even though the cortex had begun to constrict in some oocytes, RhoA still failed to accumulate at this precise site (n = 12, Fig. 4, b1–b3). A minor fraction of oocytes presented aberrant RhoA accumulation (n = 5, Fig. 4, c and d). RhoA localized normally in one fourth of the oocytes, in high correlation with the fraction of oocytes that extruded PBI.

ROCK is required for PBI extrusion

We next examined the role of ROCK, the downstream effector of Rho, during PBI emission. Oocytes were incubated in the presence of Y27632, a specific ROCK inhibitor. Y27632 reduced PBI extrusion in a dose-dependent manner (Fig. 5A). Moreover, similar to ECT2-depleted oocytes, some of the Y27632-treated oocytes that failed to extrude PBI exhibited an elongated protrusion (13.8% in the 100 μM-treated group, n = 222, Fig. 5B). The earlier stages of oocyte maturation were unaffected by the ROCK inhibitor, with all oocytes completing GVB within less than 6 h (Fig. 5C).

CDK1 phosphorylates ECT2 during oocyte maturation

Our next experiments were directed at understanding the mode of regulation of ECT2. These experiments re-

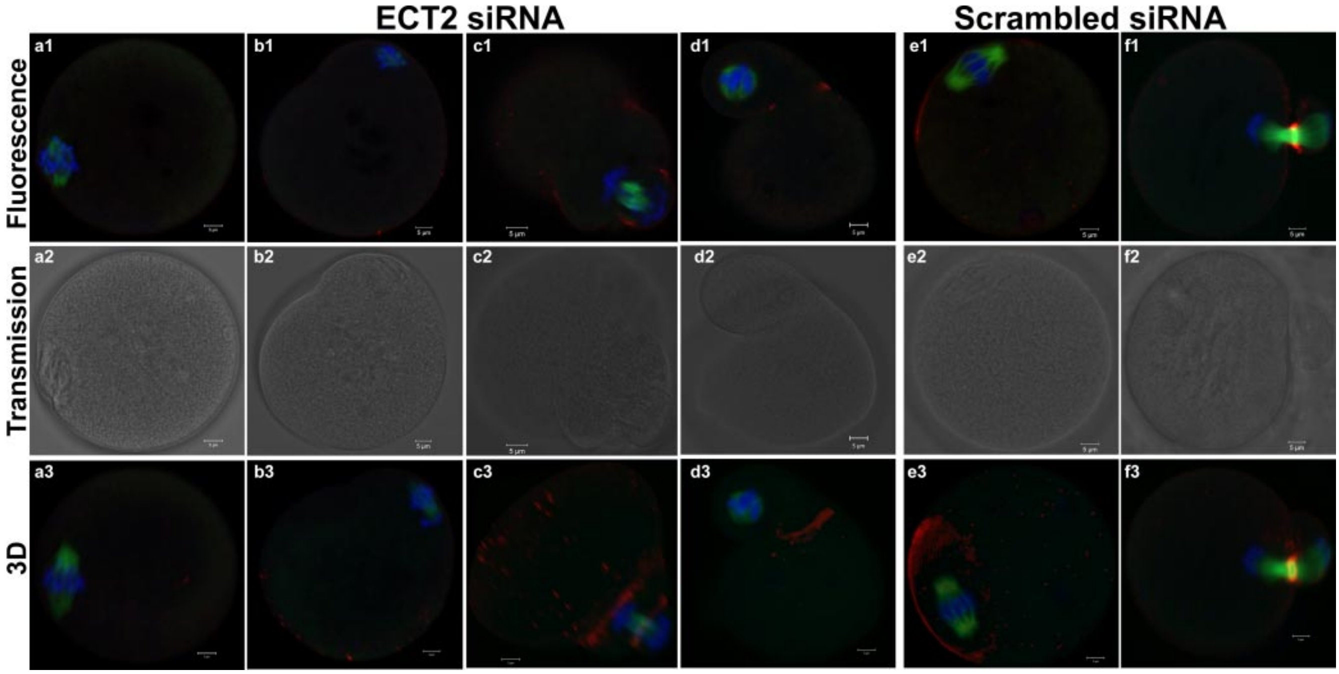

FIG. 4. RhoA localization in ECT2-depleted oocytes. Scrambled and ECT2 siRNA-microinjected oocytes were fixed during PBI emission. They were stained using RhoA (*red*) and tubulin (*green*) antibodies as well as DAPI (*blue*) and monitored by a confocal microscope. a–d and e–f, Representative photographs of oocytes microinjected with ECT2 siRNA and scrambled siRNA, respectively: a, no accumulation of RhoA was observed, and meiosis is arrested at MI stage; b, the cortex has begun to constrict, but RhoA did not accumulate at the constriction; c and d, aberrant RhoA localization and cortex constriction; e, RhoA ring-like accumulation, as in noninjected oocytes; f, constriction of RhoA ring during PBI emission.

vealed no significant change in ECT2 expression level during meiotic maturation (Fig. 6, A and B). However, a shift in ECT2 electrophoretic mobility that was previously attributed to its phosphorylation (28) was observed upon reinitiation of meiosis (Fig. 6C). This shift was partially abrogated at the onset of PBI extrusion, which occurs after approximately 12 h incubation. ECT2 electrophoretic mobility was retarded again after 24 h incubation, when the oocytes reached MII. Strikingly, the ECT2 pattern of phosphorylation described herein is in full accordance with the well-established pattern of CDK1 activity as follows: activation upon resumption of meiosis, inactivation around the time of PBI emission, and further reactivation at the MII stage (4–6). To examine whether CDK1 induces ECT2 phosphorylation at the GVB stage, we employed roscovitine, a selective CDK1 inhibitor. Oocytes were incubated for 5 h to allow the activation of CDK1 associated with their spontaneous reinitiation of meiosis. They were then transferred to a roscovitine-containing medium for 1 h. CDK1 inactivation indeed reduced the mobility shift of ECT2, observed after 6 h isolation in the nontreated oocytes (Fig. 6D). It should be noted that this effect was detected after only 1 h roscovitine treatment, suggesting that a continuous activity of CDK1 is needed to maintain ECT2 in its phosphorylated state during GVB and early MI stages.

To further establish whether CDK1 inactivation induces ECT2 dephosphorylation, CDK1 was maintained experimentally active by incubating spontaneously maturing oocytes with MG132, a potent proteasome inhibitor. We previously showed that MG132-incubated rat oocytes accumulate cyclin B and subsequently maintain a high level of CDK1 activity (9). This treatment brought about inhibition of PBI extrusion and formation of a nose-like protrusion. In the present study, this phenotype was fully reproduced; none of the MG132-treated oocytes extruded PBI, and some of them exhibited an elongated protrusion (Fig. 6F, *left*, *insets*). The electrophoretic mobility shift assay revealed that unlike the nontreated oocytes, ECT2 in the MG132-treated oocytes exhibited a retarded mobility, suggesting that CDK1 inactivation is responsible for ECT2 dephosphorylation (Fig. 6E). Because MG132 is not a MPF-specific inhibitor, a control group of oocytes was incubated in a culture medium containing the combination of MG132 and roscovitine. Under these conditions, the MG132-induced activation of CDK1, promoted by accumulation of the MPF regulatory subunit cyclin B1, should be abolished by roscovitine. Indeed, the addition of roscovitine to the MG132-treated oocytes reversed the electrophoretic mobility shift of ECT2 induced by MG132, confirming that the MG132-induced mobility shift occurred due to CDK1 prolonged activation (Fig. 6E). Taken together, these data suggest that CDK1-sustained activation is required for ECT2 phosphorylation dur-

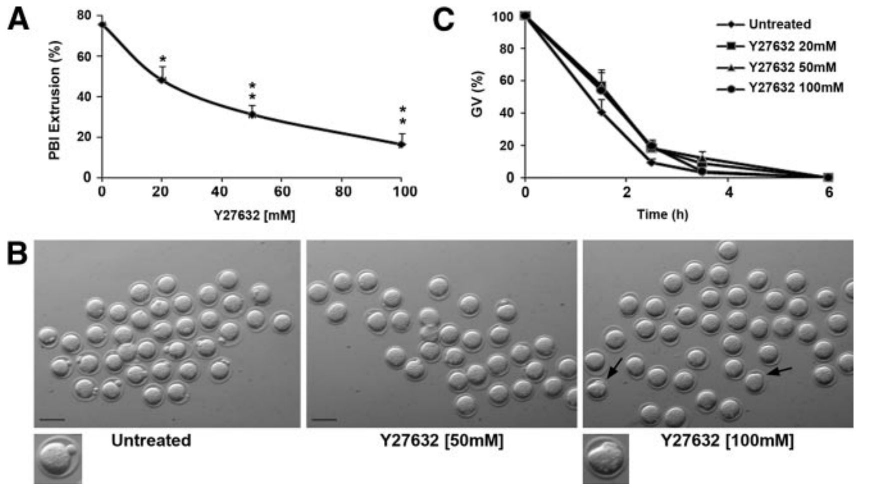

FIG. 5. Effect of the ROCK inhibitor on either PBI extrusion or GVB. Oocytes were denuded and immediately thereafter incubated with increasing concentrations of the Rho kinase (ROCK) inhibitor Y27632. A, Y27632 reduced PBI extrusion in a concentration-dependent manner. The graph shows means ± SE of four independent experiments that comprised about 55 oocytes per point per experiment. *, $P < 0.02$; **, $P < 0.0006$. B, Some of the Y27632-treated oocytes that failed to extrude a PBI exhibited an elongated protrusion (indicated by *black arrows*). C, An earlier stage of oocyte maturation, represented by GVB, was monitored at several time points. The graph presents means ± SE of three independent experiments (about 75 oocytes per point).

ing meiosis. At the onset of anaphase, CDK1 inactivation is sufficient to induce ECT2 dephosphorylation.

Discussion

We report herein that at the onset of the MI, ECT2 undergoes a CDK1-dependent phosphorylation. This is followed by its dephosphorylation upon transition to anaphase, resulting from CDK1 inactivation. In the absence of ECT2, completion of the first meiotic division is severely impaired. These oocytes, which failed to emit PBI, are either arrested at MI or contain two MII spindles, resembling binucleated somatic cells. In addition, we show that ECT2 is indispensable for RhoA translocation at the vicinity of the spindle. Finally, ROCK, the downstream effector of RhoA, mediates PBI emission.

ECT2 is required for PBI emission and its depletion results in oocytes that are either arrested at MI or contain two MII spindles

Half of the oocytes failed to complete homologous chromosome segregation (MI) in the absence of ECT2 (see model in supplemental Fig. 6B). A similar phenotype was previously described in cytochalasin D-treated oocytes (33) and in formin-2-deficient oocytes (34). In these reports, the homologous chromosomes segregated and initiated two MII spindle assembly, which then retracted and remerged rapidly back into a single spindle. What seems like an MI arrest in the ECT2-depleted oocytes could in fact represent the outcome of the above mentioned process. It should be noted that no similar phenotype was ever described in ECT2-depleted somatic cells, which may suggest that ECT2 activity may affect aspects unique to the meiotic, rather than mitotic, cell cycle.

A third of the oocytes that failed to emit PBI upon ECT2 depletion contained two MII spindles (see model in supplemental Fig. 6B). This phenomenon, which resembles binucleation in ECT2-depleted somatic cells (24, 27), has never been reported in oocytes. It apparently represents the completion of chromosome segregation that was not followed by PBI emission. Remarkably, under the conditions generated in the ooplasm in this experiment, each of the two separated sets of homologous chromosomes has formed its own stable MII spindle. Regardless of cell division failure, each spindle was aligned in parallel to the cortex, resembling the orientation of a single MII spindle during normal MII arrest. It is clear that the two well-formed MII spindles observed in the present study are not transitory structures as previously mentioned (33, 34) because they were detected 20 h after GVB.

The unique RhoA localization during PBI emission

At the onset of anaphase in mitotically dividing cells, RhoA accumulates in a ring-like manner around the spindle, preceding furrow ingression (20–23). Previous reports in somatic cells showed that RhoA promotes actin polymerization and myosin phosphorylation, thus bringing about the formation of the contractile ring (10, 12, 16). Similarly, the ring-shaped RhoA accumulation in oocytes apparently marks the localization of the future contractile ring.

Unlike somatic cells, the formation of the RhoA ring in oocytes is preceded by RhoA translocation to the cortex adjacent to the spindle, forming a dome-like structure (see model in supplemental Fig. 6A). Two hypotheses can be raised to explain the unique dome-like accumulation of RhoA in oocytes. In somatic cells, the spindle expends throughout the entire cell, enabling activation of the equatorial cortex by the centralspindlin. However, the oocyte not only is much larger than a somatic cell but also undergoes an asymmetric cell division. Under these conditions, a limited centralspindlin-cortex contact area is available. A multistep process, in which RhoA is first crudely recruited to the cortex in the vicinity of the spindle

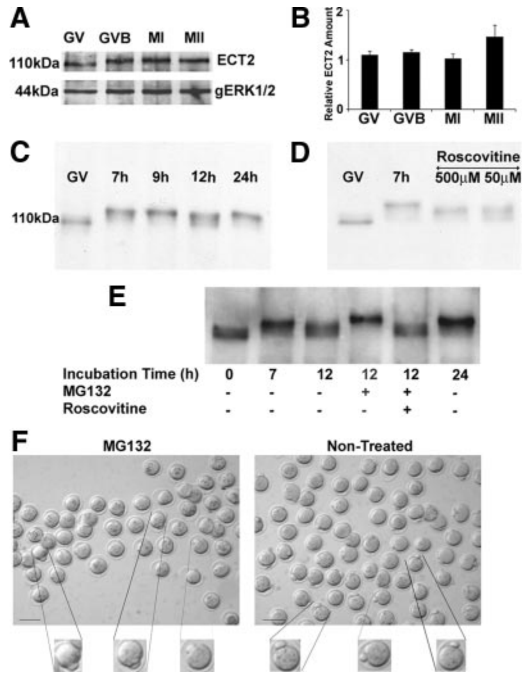

FIG. 6. CDK1 phosphorylates ECT2 upon resumption of meiosis, and its prolonged activation during anaphase I blocked ECT2 dephosphorylation as well as PBI extrusion. A, Maturing mouse oocytes (180 per lane) were extracted at 0, 4, 12, and 24 h after reinitiation of meiosis, labeled as GV, GVB, MI, and MII, respectively. The oocytes were subjected to SDS-PAGE and immunoblotted using antibodies recognizing ECT2 as well as those raised against general ERK1/2 (g-ERK1/2). B, Densitometric quantification of the results and normalization according to g-ERK1/2 protein levels. C, Maturing mouse oocytes (180 per lane), extracted at 0, 7, 9, 12, and 24 h after reinitiation of meiosis, were subjected to SDS-PAGE under conditions that allow the detection of the phosphorylation shift (see *Materials and Methods*) and were immunoblotted with anti-ECT2 antibodies. D, Oocytes were allowed to mature spontaneously. After 5 h, they were incubated in either roscovitine (500 and 50 μM) or vehicle for 1 h. A negative control included meiotically arrested oocytes. The extracts were subjected to SDS-PAGE and immunoblotted with anti-ECT2 antibodies. E, Oocytes were allowed to mature spontaneously. After 7 h, they were transferred for incubation without or with either MG132 (10 μM) in the presence or absence of roscovitine (100 μM). After an additional 5 h, the oocytes were frozen. Meiotically arrested oocytes and oocytes after 7 h spontaneous maturation served as references for ECT2 dephosphorylated and phosphorylated forms, respectively. The extracts were subjected to SDS-PAGE and immunoblotted with anti-ECT2 antibodies. F, A representative photograph of MG132-treated and nontreated groups of oocytes, 24 h after isolation. *Bars*, 100 μm. A–E, Representative result of three similar individual experiments displaying similar results.

to form a dome-like accumulation and later reorganizes into the functional ring, may be particularly adapted to fit the oocyte properties. The GTPase flux model, which provides evidence for the considerable plasticity of the RhoA zone, easily explains the remodeling of the RhoA shape (35–37). The second explanation for the requirement of a dome-like accumulation in oocytes takes into account the polarity of the cortex of the extruding PBI. The RhoA accumulation at the region of the cortex that is adjacent to the spindle may be a prerequisite for further cortex polarization. Supporting this hypothesis, CDC42 activation, which controls PBI outpocketing, requires RhoA activation (30). Further research is necessary to examine these hypotheses.

Role of ROCK in PBI emission

The downstream effector of RhoA, ROCK, is one of the kinases that phosphorylates the myosin II regulatory light chain during cytokinesis, inducing constriction of the actomyosin ring. In agreement with a previous publication (38), we show herein that ROCK inhibition blocks PBI extrusion. This finding is somewhat unexpected because depletion of both ROCK-I and ROCK-II isoforms in HeLa cells induced only a minor increase in the multinucleation incidence, suggesting that ROCK is not necessary for cytokinesis in somatic cells (16, 20, 39). This discrepancy can be explained by a redundant mechanism responsible for the activation of myosin II in somatic cells. In addition, an adhesion-mediated cell division pathway that bypasses the myosin-induced cell division, has been suggested to explain the dispensability of ROCK in somatic cells (40, 41). However, because the oocytes do not adhere to the substrate, this adhesion-dependent pathway evidently does not exist. Furthermore, the absolute requisite of ROCK for PBI emission denies the presence of another kinase that would activate myosin II in oocytes.

Unlike previous studies suggesting that ROCK is also involved in an early stage of meiosis maturation, inhibition of this kinase in our hands had no effect on GVB (38, 42). Our finding indicates that the ECT2-RhoA-ROCK pathway is not active during early meiosis, supporting the assumption that up to metaphase, ECT2 is maintained in a phosphorylated inactive state, avoiding premature cytokinesis.

CDK1 regulates the ECT2 phosphorylation state

We demonstrate herein, for the first time, that ECT2 is subjected to phosphorylation/dephosphorylation throughout meiosis in oocytes. We reveal that PBI emission is temporally associated with ECT2 dephosphorylation. Interestingly, the phosphorylation state of ECT2 is tightly correlated with the pattern of CDK1 activity. Furthermore, our data provide the first demonstration that an active CDK1 phosphorylates ECT2 during the first meiotic metaphase and that CDK1 inactivation upon anaphase allows ECT2 dephosphorylation.

Previous studies in mitosis have demonstrated the importance of the initial ECT2 phosphorylation (28, 29). The added value of our experiment is the indication that a prolonged activity of CDK1 is required to maintain a phosphorylated ECT2. A plausible explanation for the requirement of continuously active CDK1 would be that ECT2 is permanently subjected to dephosphorylation by a specific phosphatase, and therefore, a sustained kinase activity is necessary to maintain it in a phosphorylated state. This kinetics assessment of the CDK1-induced ECT2 phosphorylation could be analyzed in oocytes due to the substantial longer duration of meiosis compared with mitosis.

The question whether CDK1 inactivation generates the sufficient condition to induce ECT2 dephosphorylation was never assessed in cell cycle studies. In this study, we provide evidence that it is the inactivation of CDK1 that allows ECT2 dephosphorylation. Since ECT2 is known to be regulated by its phosphorylation, we suggest that CDK1 inactivation induces PBI emission via ECT2 dephosphorylation and its subsequent activation.

ECT2 displays an interesting pattern of phosphorylation/dephosphorylation. It is phosphorylated at prometaphase/metaphase, dephosphorylated at the metaphase-to-anaphase transition, and rephosphorylated during MII arrest. A similar pattern of phosphorylation was observed for several other proteins such as protein regulator of cytokinesis 1 (PRC1), mitotic kinesin-like protein-1 (MKLP1), and cell division cycle20 homolog1 (CDH1), which play a critical role during cytokinesis (43–45). Their phosphorylation by CDK1 during metaphase inhibits cytokinesis, whereas their dephosphorylation during anaphase, upon CDK1 inactivation, permits cell division. This mechanism ensures that cytokinesis occurs at the appropriate time point during the cell cycle, avoiding aneuploidy. We therefore suggest that ECT2 is regulated in a similar mode: the CDK1 phosphorylation-mediated inactivation at MI is followed by a dephosphorylation-dependent activation at the first anaphase. According to this model, the balance between the phosphorylated and dephosphorylated states provides a tight regulation on ECT2 activity. This hypothesis assumes that the phosphorylated ECT2 is inactive. Interestingly, subsequent to PBI emission, ECT2 is rephosphorylated. This event is presumably responsible for its inactivation that would apparently prevent premature extrusion of the second PB. Supporting this idea, only dephosphorylated ECT2 was shown to interact with the centralspindlin component Rac GTPase-activating protein 1 RACGAP1, also known as CYK-4, which is required for completion of cytokinesis (23). However, in disagreement to this theory, phosphorylated and dephosphorylated ECT2 were both reported active and localized properly during cytokinesis (29). Further investigations are needed to elucidate the phosphorylation requirement for ECT2 activity.

In conclusion, our results demonstrate the necessity of the ECT2-RhoA-ROCK pathway for PBI emission in mammalian oocytes. This pathway appears to be turned on at anaphase I, upon CDK1 inactivation. In part of the ECT2-depleted oocytes, the homologous chromosomes have separated, generating oocytes that contain two MII spindles. Those oocytes that did not generate two spindles seemed to be arrested at MI. Furthermore, ECT2 triggers the formation of the RhoA ring. RhoA further activates its effector ROCK, which, by phosphorylating the myosin light chain, induces constriction of the contractile ring and the subsequent PBI emission.

Acknowledgments

We thank Y. Shahar for critical reading and helpful discussions.

Address all correspondence and requests for reprints to: Prof. Nava Dekel, Weizmann Institute of Science, Department of Biological Regulation, Herzel Street 1, Rehovot 76100, Israel. E-mail: nava.dekel@weizmann.ac.il.

This study was supported by the Dwek Fund for Biomedical Research. Professor Nava Dekel is the incumbent of the Philip M. Klutznick Professorial Chair in Developmental Biology.

Disclosure Summary: The authors have nothing to disclose.

References

1. **Gautier J, Minshull J, Lohka M, Glotzer M, Hunt T, Maller JL** 1990 Cyclin is a component of maturation-promoting factor from *Xenopus*. Cell 60:487–494
2. **Gautier J, Norbury C, Lohka M, Nurse P, Maller J** 1988 Purified maturation-promoting factor contains the product of a *Xenopus* homolog of the fission yeast cell cycle control gene cdc2+. Cell 54:433–439
3. **Masui Y, Markert CL** 1971 Cytoplasmic control of nuclear behavior during meiotic maturation of frog oocytes. J Exp Zool 177:129–145
4. **Choi T, Aoki F, Mori M, Yamashita M, Nagahama Y, Kohmoto K** 1991 Activation of p34cdc2 protein kinase activity in meiotic and mitotic cell cycles in mouse oocytes and embryos. Development 113: 789–795
5. **Gavin AC, Cavadore JC, Schorderet-Slatkine S** 1994 Histone H1 kinase activity, germinal vesicle breakdown and M phase entry in mouse oocytes. J Cell Sci 107(Pt 1):275–283
6. **Josefsberg LB, Galiani D, Lazar S, Kaufman O, Seger R, Dekel N** 2003 Maturation-promoting factor governs mitogen-activated protein kinase activation and interphase suppression during meiosis of rat oocytes. Biol Reprod 68:1282–1290
7. **Winston NJ** 1997 Stability of cyclin B protein during meiotic maturation and the first mitotic cell division in mouse oocytes. Biol Cell 89:211–219
8. **Glotzer M, Murray AW, Kirschner MW** 1991 Cyclin is degraded by the ubiquitin pathway. Nature 349:132–138
9. **Josefsberg LB, Galiani D, Dantes A, Amsterdam A, Dekel N** 2000 The proteasome is involved in the first metaphase-to-anaphase transition of meiosis in rat oocytes. Biol Reprod 62:1270–1277
10. **Kishi K, Sasaki T, Kuroda S, Itoh T, Takai Y** 1993 Regulation of cytoplasmic division of *Xenopus* embryo by rho p21 and its inhibitory GDP/GTP exchange protein (rho GDI). J Cell Biol 120:1187–1195
11. **Kosako H, Goto H, Yanagida M, Matsuzawa K, Fujita M, Tomono Y, Okigaki T, Odai H, Kaibuchi K, Inagaki M** 1999 Specific accumulation of Rho-associated kinase at the cleavage furrow during

cytokinesis: cleavage furrow-specific phosphorylation of intermediate filaments. Oncogene 18:2783–2788
12. **Madaule P, Eda M, Watanabe N, Fujisawa K, Matsuoka T, Bito H, Ishizaki T, Narumiya S** 1998 Role of citron kinase as a target of the small GTPase Rho in cytokinesis. Nature 394:491–494
13. **Glotzer M** 2005 The molecular requirements for cytokinesis. Science 307:1735–1739
14. **Pelham RJ, Chang F** 2002 Actin dynamics in the contractile ring during cytokinesis in fission yeast. Nature 419:82–86
15. **Kimura K, Ito M, Amano M, Chihara K, Fukata Y, Nakafuku M, Yamamori B, Feng J, Nakano T, Okawa K, Iwamatsu A, Kaibuchi K** 1996 Regulation of myosin phosphatase by Rho and Rho-associated kinase (Rho-kinase). Science 273:245–248
16. **Kosako H, Yoshida T, Matsumura F, Ishizaki T, Narumiya S, Inagaki M** 2000 Rho-kinase/ROCK is involved in cytokinesis through the phosphorylation of myosin light chain and not ezrin/radixin/moesin proteins at the cleavage furrow. Oncogene 19:6059–6064
17. **Matsumura F** 2005 Regulation of myosin II during cytokinesis in higher eukaryotes. Trends Cell Biol 15:371–377
18. **Drechsel DN, Hyman AA, Hall A, Glotzer M** 1997 A requirement for Rho and Cdc42 during cytokinesis in *Xenopus* embryos. Curr Biol 7:12–23
19. **O'Connell CB, Wheatley SP, Ahmed S, Wang YL** 1999 The small GTP-binding protein rho regulates cortical activities in cultured cells during division. J Cell Biol 144:305–313
20. **Kamijo K, Ohara N, Abe M, Uchimura T, Hosoya H, Lee JS, Miki T** 2006 Dissecting the role of Rho-mediated signaling in contractile ring formation. Mol Biol Cell 17:43–55
21. **Kimura K, Tsuji T, Takada Y, Miki T, Narumiya S** 2000 Accumulation of GTP-bound RhoA during cytokinesis and a critical role of ECT2 in this accumulation. J Biol Chem 275:17233–17236
22. **Yoshizaki H, Ohba Y, Parrini MC, Dulyaninova NG, Bresnick AR, Mochizuki N, Matsuda M** 2004 Cell type-specific regulation of RhoA activity during cytokinesis. J Biol Chem 279:44756–44762
23. **Yüce O, Piekny A, Glotzer M** 2005 An ECT2-centralspindlin complex regulates the localization and function of RhoA. J Cell Biol 170:571–582
24. **Bement WM, Benink HA, von Dassow G** 2005 A microtubule-dependent zone of active RhoA during cleavage plane specification. J Cell Biol 170:91–101
25. **Chalamalasetty RB, Hümmer S, Nigg EA, Silljé HH** 2006 Influence of human Ect2 depletion and overexpression on cleavage furrow formation and abscission. J Cell Sci 119:3008–3019
26. **Nishimura Y, Yonemura S** 2006 Centralspindlin regulates ECT2 and RhoA accumulation at the equatorial cortex during cytokinesis. J Cell Sci 119:104–114
27. **Prokopenko SN, Brumby A, O'Keefe L, Prior L, He Y, Saint R, Bellen HJ** 1999 A putative exchange factor for Rho1 GTPase is required for initiation of cytokinesis in *Drosophila*. Genes Dev 13:2301–2314
28. **Tatsumoto T, Xie X, Blumenthal R, Okamoto I, Miki T** 1999 Human ECT2 is an exchange factor for Rho GTPases, phosphorylated in G2/M phases, and involved in cytokinesis. J Cell Biol 147:921–928
29. **Hara T, Abe M, Inoue H, Yu LR, Veenstra TD, Kang YH, Lee KS, Miki T** 2006 Cytokinesis regulator ECT2 changes its conformation through phosphorylation at Thr-341 in G2/M phase. Oncogene 25:566–578
30. **Zhang X, Ma C, Miller AL, Katbi HA, Bement WM, Liu XJ** 2008 Polar body emission requires a RhoA contractile ring and Cdc42-mediated membrane protrusion. Dev Cell 15:386–400
31. **Tsafriri A, Chun SY, Zhang R, Hsueh AJ, Conti M** 1996 Oocyte maturation involves compartmentalization and opposing changes of cAMP levels in follicular somatic and germ cells: studies using selective phosphodiesterase inhibitors. Dev Biol 178:393–402
32. **Yonemura S, Hirao-Minakuchi K, Nishimura Y** 2004 Rho localization in cells and tissues. Exp Cell Res 295:300–314
33. **Kubiak J, Paldi A, Weber M, Maro B** 1991 Genetically identical parthenogenetic mouse embryos produced by inhibition of the first meiotic cleavage with cytochalasin D. Development 111:763–769
34. **Verlhac MH, Lefebvre C, Guillaud P, Rassinier P, Maro B** 2000 Asymmetric division in mouse oocytes: with or without Mos. Curr Biol 10:1303–1306
35. **Bement WM, Miller AL, von Dassow G** 2006 Rho GTPase activity zones and transient contractile arrays. Bioessays 28:983–993
36. **Miller AL, Bement WM** 2009 Regulation of cytokinesis by Rho GTPase flux. Nat Cell Biol 11:71–77
37. **Miller AL, von Dassow G, Bement WM** 2008 Control of the cytokinetic apparatus by flux of the Rho GTPases. Biochem Soc Trans 36:378–380
38. **Zhong ZS, Huo LJ, Liang CG, Chen DY, Sun QY** 2005 Small GTPase RhoA is required for ooplasmic segregation and spindle rotation, but not for spindle organization and chromosome separation during mouse oocyte maturation, fertilization, and early cleavage. Mol Reprod Dev 71:256–261
39. **Yokoyama T, Goto H, Izawa I, Mizutani H, Inagaki M** 2005 Aurora-B and Rho-kinase/ROCK, the two cleavage furrow kinases, independently regulate the progression of cytokinesis: possible existence of a novel cleavage furrow kinase phosphorylates ezrin/radixin/moesin (ERM). Genes Cells 10:127–137
40. **Kanada M, Nagasaki A, Uyeda TQ** 2005 Adhesion-dependent and contractile ring-independent equatorial furrowing during cytokinesis in mammalian cells. Mol Biol Cell 16:3865–3872
41. **Zang JH, Cavet G, Sabry JH, Wagner P, Moores SL, Spudich JA** 1997 On the role of myosin-II in cytokinesis: division of *Dictyostelium* cells under adhesive and nonadhesive conditions. Mol Biol Cell 8:2617–2629
42. **Cheon YP, Kim SW, Kim SJ, Yeom YI, Cheong C, Ha KS** 2000 The role of RhoA in the germinal vesicle breakdown of mouse oocytes. Biochem Biophys Res Commun 273:997–1002
43. **Mishima M, Pavicic V, Grüneberg U, Nigg EA, Glotzer M** 2004 Cell cycle regulation of central spindle assembly. Nature 430:908–913
44. **Reis A, Chang HY, Levasseur M, Jones KT** 2006 APCcdh1 activity in mouse oocytes prevents entry into the first meiotic division. Nat Cell Biol 8:539–540
45. **Zhu C, Lau E, Schwarzenbacher R, Bossy-Wetzel E, Jiang W** 2006 Spatiotemporal control of spindle midzone formation by PRC1 in human cells. Proc Natl Acad Sci USA 103:6196–6201